

Enhanced thermal response of phase change materials using optimized fin geometries in a dual-enclosure heat storage unit

Vignesh Elangovan^a, Ramanipriya Mahalingam^a, Mohammad Junaid^b, Goutam Saha^{c,d,*}

^a Department of Mathematics, PSG Institute of Technology and Applied Research, Neelambur-641 062, India

^b Department of Mechanical Engineering, Shahjalal University of Science and Technology, Sylhet 3114, Bangladesh

^c Department of mathematics, University of Dhaka, Dhaka 1000, Bangladesh

^d Miyan Research Institute, International University of Business Agriculture and Technology, Uttara, Dhaka 1230, Bangladesh

ARTICLE INFO

Keywords:

Phase Change Material (PCM)

Enthalpy–Porosity Method

Thermal Energy Storage

Chamfered Dual-Enclosure

Geometric Enhancement

Thermal Response Time

ABSTRACT

The inherently low thermal conductivity of phase change materials (PCMs) poses a significant limitation to the performance of latent heat thermal energy storage (LHTES) systems. This study presents a comprehensive numerical investigation into the melting behavior of RT-27 PCM within a two-dimensional chamfered dual-enclosure, equipped with internal and external aluminum fins of four distinct geometries: rectangular, triangular, U-shaped, and wavy. The system is subjected to constant heat fluxes of 500, 1000, 1500, and 2000 W/m². The enthalpy–porosity method is employed in ANSYS Fluent 2021 to solve the governing equations, and model validation is performed against experimental data to ensure reliability. Results demonstrate that fin geometry substantially influences melting rate, thermal uniformity, and energy storage efficiency. At a heat flux of 1000 W/m², the U-shaped fin achieved complete melting in 2000 s, with an average temperature of 365 K and stored energy of ~160 kJ/kg. In contrast, the triangular fin exhibited the slowest response, completing melting in 2700 s with a lower average temperature of 315 K and energy storage of ~75 kJ/kg. Increasing heat flux to 2000 W/m² reduced melting time to 1400 s in the U-shaped configuration, confirming its superior thermal performance. The wavy and rectangular fins also showed favorable results, balancing thermal response and uniformity. The findings confirm that the integration of U-shaped and rectangular fins enhances heat propagation, reduces phase-change duration, and improves energy storage capacity. These insights provide a strategic framework for designing compact, high-efficiency LHTES systems for applications in energy, electronics, and thermal management technologies.

1. Introduction

Phase Change Materials (PCMs) absorb or release thermal energy during phase transitions, making them valuable for both heating and cooling applications. These materials are especially effective for storing winter cold and improving building thermal management. PCMs are generally categorized into organic compounds and salt hydrates. With the increasing use of renewable energy and challenges like intermittent supply and peak demand, PCMs are gaining widespread use in building heating and cooling systems—their largest market. Beyond buildings, PCMs also serve in solar cooking, cold-energy storage for batteries, waste heat recovery, and reducing dependence on electricity and diesel generators.

Numerous studies have investigated methods to enhance PCM thermal performance. Zhao et al [1] examined the melting behavior of PCM in a rectangular enclosure heated from the base, analyzing the impact of fin spacing and optimizing fin lengths for aluminum and stainless steel. Their findings demonstrated strong agreement between numerical and experimental results. Similarly, César O. Oliveski et al [2] analyzed the melting of lauric acid in a rectangular cavity with 78 fin configurations while maintaining constant mass and surface area. Using finite-volume CFD simulations, they concluded that longer fins with optimized aspect ratios significantly reduced melting times. The addition of copper fins to a square cell containing paraffin wax RT42 was shown to improve the heat charging rate, reducing melting time by 22.22 %, 33.33 %, and 55.56 % for different finned setups compared to a no-fin scenario. Khadim et al [3] demonstrated that placing fins on the same wall as the

* Corresponding author.

E-mail addresses: vigneshpsg67@gmail.com (V. Elangovan), mahalingamramanipriya@gmail.com (R. Mahalingam), md.junaid.jkr@gmail.com (M. Junaid), gsahamath@du.ac.bd (G. Saha).

<https://doi.org/10.1016/j.ctta.2025.100218>

Received 1 August 2025; Received in revised form 29 August 2025; Accepted 31 August 2025

Available online 1 September 2025

2667-3126/© 2025 The Authors. Published by Elsevier B.V. CCBY-NC license This is an open access article under the CC BY-NC license (<http://creativecommons.org/licenses/by-nc/4.0/>).

Nomenclature			
Symbols		Q	Heat flux (W/m^2)
C_p	Specific heat (kJ/kg K)	A_{mush}	Mushy zone constant ($\text{kg/m}^3 \text{ s}$)
\vec{g}	Gravitational acceleration (m/s^2)	\vec{v}	Velocity vector (m/s)
k	Thermal conductivity (W/m K)	t	Time (s)
P	Pressure (Pa)	Greek letters	
T	Temperature ($^{\circ}\text{C}$)	γ	Liquid fraction
T_{ref}	Reference temperature ($^{\circ}\text{C}$)	μ	Dynamic viscosity (kg/m s)
T_m	Melting point ($^{\circ}\text{C}$)	ρ	Density solid/liquid (kg/m^3)
T_l	Liquidus temperature ($^{\circ}\text{C}$)	β	Thermal expansion coefficient ($1/\text{K}$)
T_s	Solidus temperature ($^{\circ}\text{C}$)	δ	A small number (0.001) used to avoid division by zero
L_h	Latent heat of fusion (kJ/kg)	Subscript	
h	Sensible enthalpy (kJ/kg)	l	Liquid
H	Total enthalpy (kJ/kg)	s	Solid
ΔH	Latent heat (kJ/kg)	avg	Average

heat source—especially on the left wall—yielded the most efficient heat transfer, making this configuration beneficial for enhancing solar energy system performance. Chen et al [4] used inverse computational fluid dynamics (CFD) and experimental analysis to study fluid flow and heat transfer in square cavities equipped with rectangular fins. They introduced a heat sink containing paraffin-based PCM to enhance thermal dissipation and examined how varying PCM height influences heat absorption.

Rawat et al [5] explored the enhancement of PCM melting within a rectangular enclosure using flanged fins. Their study assessed various fin length ratios and materials, including copper, aluminum, and carbon steel. The results showed that a lower L_u/L_d ratio, when combined with materials of high thermal conductivity, significantly accelerated the melting process. Among the tested configurations, copper fins with a 0.25 L_u/L_d ratio achieved the fastest melting, lowest melting time (t_m), and the minimum specific heat capacity weighted average ($C_{p,w}$). Elsayed [6] conducted a numerical investigation of PCM melting inside triangular cylinder containers using commercial paraffin wax and heated air streams. The study analyzed flow behavior, convective heat transfer, and heat storage capacity across different container geometries. Simulations were carried out in ANSYS Fluent using the SIMPLE algorithm. Findings highlighted that the apex angle and base length of the triangular containers had a significant impact on surface temperature distribution and overall thermal storage efficiency. Fin structure configuration and PCM placement were also identified as key factors influencing melting performance, particularly by reducing melting time and enhancing heat transfer rates. In a related study, Hong et al [7] evaluated the integration of latent heat thermal energy storage (LHTES) units with solar receivers and photovoltaic thermal management systems, emphasizing their potential to boost system efficiency. Additionally, Qasem et al [8] investigated the thermal performance of PCMs with eight different T-fin placements. Their results showed that the location of the fins plays a crucial role in the melting process, with fins positioned near the upper section of the chamber significantly improving the melting rate.

Although PCMs are widely used for thermal energy storage, their effectiveness is often limited by slow melting and solidification rates. To address this, Kiyak et al [9] proposed a novel strategy combining cyclic heating and cooling with various fin shapes and orientations. Their results showed that this approach significantly reduces melting time, enhances energy storage capacity, and improves energy recovery, thereby boosting the overall efficiency of PCM-based thermal storage systems. Czerwiński and Wołoszyn [10] analyzed the impact of different partition configurations on phase change duration using Fluent 2021R2. They found that combining vertical tubes with horizontal partitions resulted in the shortest melting and solidification times, as well as the highest

specific enthalpy changes. Their study emphasized the importance of partition thermal conductivity in achieving a more uniform temperature distribution, which facilitates consistent heat extraction and supply. Barthwal and Rakshit [11] studied the melting behavior of PCM in two-dimensional rectangular enclosures designed for photovoltaic thermal systems. They evaluated three distinct fin configurations and found that triangular and Y-type fins delayed melting, while equal and increasing-stepped Y-fin arrangements produced the highest time enhancement ratios, indicating improved thermal performance. Similarly, Tan et al [12] examined the melting characteristics of PCM within rectangular enclosures incorporating different fin geometries. Their findings confirmed that modifying fin shapes can significantly improve heat transfer rates and overall efficiency of latent heat storage systems.

Zhao et al [13] investigated two-phase flow boiling in staggered pin-finned channels using the Mixture multiphase model. The study compared different fin cross-sectional shapes to assess their impact on heat transfer, pressure drop, and temperature uniformity under varying heat flux conditions. Among the tested configurations, pentagonal fins exhibited the highest overall thermal performance. Hammoodi et al [14] analyzed the influence of an air layer on the melting behavior of paraffin wax RT42 PCM in a hemicylindrical enclosure using ANSYS Fluent 16 and the enthalpy-porosity method. Three air layer thicknesses were considered, with results showing that a 1 mm layer extended melting time by 125 %, while a 2 mm layer increased it by 225 %. These findings highlight the substantial impact of ambient air layers on the charging efficiency of thermal energy storage systems. Zhang et al [15] studied the effect of the connection angle of an I-shaped fin on melting and solidification in a vertical PCM unit. An angle of 30° reduced melting time by 14 %, enhanced solidification by 45 %, and achieved a 32 % improvement in the melting performance, marking it as the most efficient configuration. Liu et al [16] numerically explored the effect of non-uniform longitudinal fins placed near the bottom of a heated side-wall enclosure containing RT42. The goal was to boost natural convection during the final melting stages. Results indicated that lower-region fin placement significantly improved energy storage efficiency, shortened total melting time, increased energy storage rate, and elevated the average Nusselt number. Kiyak et al [17] examined the thermal performance of a PCM-filled energy storage unit, focusing on the effects of heater and cooler placement as well as two distinct geometric configurations. Their findings showed that side heating significantly accelerates the melting process, while top cooling combined with a square geometry enhances solidification efficiency. The study suggests that future research should explore more intricate geometries and a broader selection of PCM materials to further optimize thermal behavior.

Curved enclosures, frequently found in natural systems, latent heat storage units, metal furnaces, and thermal control devices, are

particularly effective for PCM applications. Osman et al [18] conducted both experimental and numerical investigations on Rayleigh–Bénard convection in semi-circular enclosures, highlighting their favorable thermal performance in such configurations. Rahmani et al [19] utilized the lattice Boltzmann method to study magnetohydrodynamic (MHD) flow and PCM melting within a battery pack. Their results revealed that MHD forces significantly affect the melting process, with direct implications for improving thermal management, performance, and safety in battery systems. Liu et al [20] introduced a heptahedron-shaped energy storage enclosure designed to enhance natural convection and reduce PCM melting time. The design features strategic variations in volume—expanded at the top and bottom, and reduced near the right wall. Three-dimensional numerical simulations demonstrated that the heptahedron configuration effectively prolongs the dominant melting phase, intensifies natural convection, and mitigates unfavorable thermal effects typically seen at enclosure corners. Wagh and Saha [21] proposed a hybrid cooling strategy for lithium-ion batteries (LIBs) that integrates PCMs with active cooling to achieve a more uniform temperature distribution and improve PCM solidification recovery time. This approach effectively lowers the peak battery temperature, accelerates the recovery of the PCM phase, and enhances the overall reliability of the system under extreme ambient conditions. Souayfane et al [22] examined the rising cooling demand in buildings and highlighted the benefits of integrating PCMs into thermal energy storage systems. Their study emphasized PCMs' ability to reduce peak cooling loads, enable downsizing of HVAC systems, and maintain indoor comfort, while also noting performance limitations under extreme summer conditions.

Nejman and Cieślak [23] investigated how heating and cooling rates affect the thermal behavior of polyester materials embedded with microencapsulated PCMs (MPCMs). They found that faster thermal cycling raised melting points, lowered crystallization points, and altered enthalpy values depending on MPCM type. Bista et al [24] explored the use of PCMs in vapor compression refrigeration systems to boost efficiency, cut energy use, and ensure thermal stability across multiple cycles. PCMs were integrated into components like the evaporator, condenser, and compartments, resulting in enhanced system performance. Lee et al [25] developed a PCM-based heat sink for high-power electronic devices, incorporating fins, metal foams, and nanoparticles to improve energy efficiency and ensure silent operation under high thermal loads. The optimized design effectively reduced surface temperatures and enhanced thermal reliability. Ahmed et al [26] investigated thermal management strategies for tablet PCs using PCMs encapsulated in thin aluminized laminated film. Their findings showed that the PCM-based thermal energy storage unit effectively reduced temperature spikes during transient start-up, resulting in a lower overall operating temperature. As tablet designs become increasingly thin, lightweight, and compact, efficient thermal regulation becomes essential. Similarly, Marin et al [27] evaluated a PCM-based thermal energy storage system integrated into a tablet PC, also using thin aluminized laminated film. Their results confirmed the system's effectiveness in managing heat loads in compact electronics. Bondareva and Sheremet [28] analyzed the cooling and heat storage performance of PCMs combined with

melting time was highly dependent on the length and width of the profile fins.

Novelty of the study:

This study addresses a critical gap in understanding the thermal behavior of PCMs by examining the impact of heated wall configurations within a PCM-filled cavity. The primary objective is to investigate how different heated wall geometries influence key thermal performance indicators, such as liquid fraction, melting time, and energy storage capacity. A numerical approach based on the enthalpy-porosity method is employed to analyze the melting characteristics of RT-27 PCM within a uniquely designed chamfered dual enclosure. The study also evaluates the effect of varying heat flux conditions applied to each wall configuration, aiming to uncover the interplay between wall geometry and heat input on PCM performance. The findings are expected to provide valuable insights for optimizing heated wall designs, contributing to the advancement of efficient and reliable thermal energy storage systems.

1.1. Physical model

A two-dimensional, chamfered, dual-enclosure system containing PCMs is investigated to evaluate thermal performance under different fin geometries. The system has the following dimensions: total height (H) = 20 mm, chamfered height (H_c) = 5 mm, total length (L) = 20 mm, and chamfered length (L_c) = 5 mm. The bottom, right, and top walls of the cavity are thermally insulated, effectively preventing any heat exchange through these boundaries. A constant heat flux (Q) is applied along the left vertical wall, which incorporates four different externally attached fin geometries: rectangular, triangular, U-shaped, and wavy. Additionally, a solid aluminum fin of uniform thickness (0.5 mm) is placed diagonally inside the cavity to enhance internal heat distribution. The internal diagonal fin is intended to act as a thermal bridge and plume guide; synergy with the wall-mounted fin is evaluated qualitatively via spatiotemporal LF and temperature fields and formalized through time- and uniformity-based synergy indices. The PCM selected for this study is RT-27, known for its favorable melting characteristics and latent heat storage capacity, while aluminum is used for the fins due to its high thermal conductivity. A detailed comparison is conducted for each geometric configuration to examine the influence of fin shape on melting behavior and heat transfer characteristics. The thermophysical properties of the materials used in this study are presented in Junaid et al [29] Fig. 1.

2. Mathematical modelling

The numerical approach to the melting process employed the enthalpy-porosity model, a technique that equals liquid fraction. Several assumptions are necessary for numerical model development which are stated in Junaid et al [29].

Governing equations are presented below [29]:

$$\frac{\partial \rho}{\partial t} + \nabla \cdot (\rho \vec{v}) = 0 \quad (1a)$$

$$\frac{\partial}{\partial t} (\rho \vec{v}) + \vec{v} \cdot \nabla (\rho \vec{v}) = -\nabla p + \mu \nabla^2 \vec{v} + \rho \beta \vec{g} (T - T_{ref}) + \frac{(1 - \gamma)^2}{(\gamma^3 + \delta)} A_{mush} \vec{v} \quad (1b)$$

heat-spreading metal slabs in electronic systems. They focused on how fin profile shapes influence convective flow patterns and PCM melting dynamics, providing hydrodynamic and thermodynamic characteristics across different melting stages. The study found that complete PCM

$$\frac{\partial}{\partial t} (\rho H) + \nabla \cdot (\rho \vec{v} H) = \nabla \cdot (k_{eff} \nabla T) \quad (1c)$$

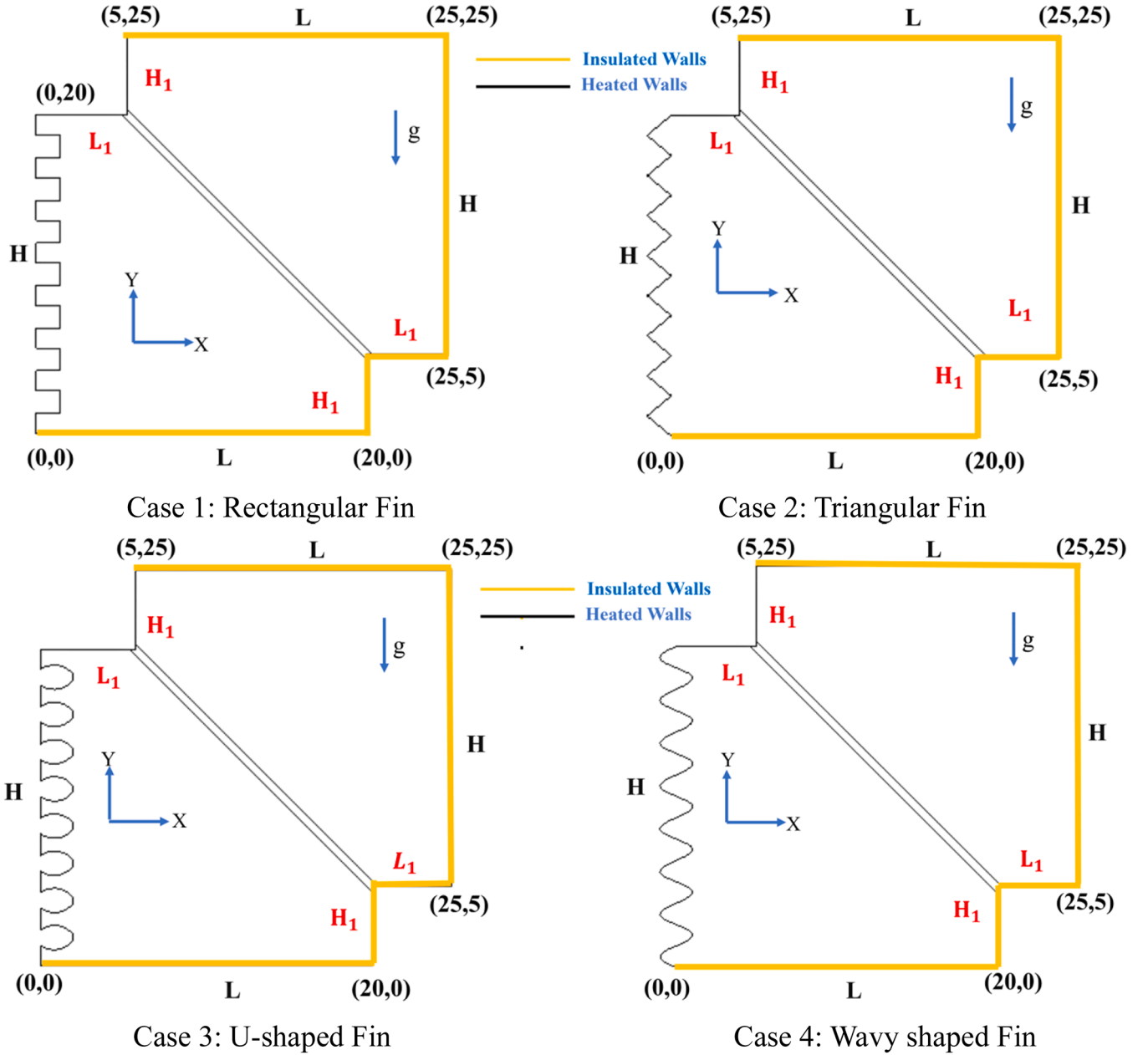


Fig. 1. Schematic diagram of the domain.

Total enthalpy (H) in Eq. (1c) is calculated using Eq. (2) [29,30]:

$$H = h + \Delta H \quad (2a)$$

$$h = h_{ref} + \int_{T_{ref}}^T C_p \Delta T \quad (2b)$$

$$\Delta H = \gamma L \quad (2c)$$

In Eqs. (2–4), h and ΔH are sensible enthalpy and latent heat change respectively. Also, h_{ref} corresponds to sensible enthalpy at a reference temperature T_{ref} . L is latent heat of PCM.

The liquid fraction γ can be determined using Eq. (3) [29,30]:

$$\gamma = \begin{cases} 0 & \text{if } T < T_s \\ \frac{T - T_s}{T_l - T_s} & \text{if } T_s < T < T_l \\ 1 & \text{if } T_l < T \end{cases} \quad (3)$$

Initial and Boundary Conditions

All walls : $u = v = 0 \text{ m/s}$

All the left walls : $Q = 1000 \text{ W/m}^2$

Remaining walls : Insulated

Internal Fin : No – slip condition

(4)

3. Numerical methods

In this study, ANSYS Fluent 2021 is utilized to solve the governing equations along with the specified boundary conditions. The simulation

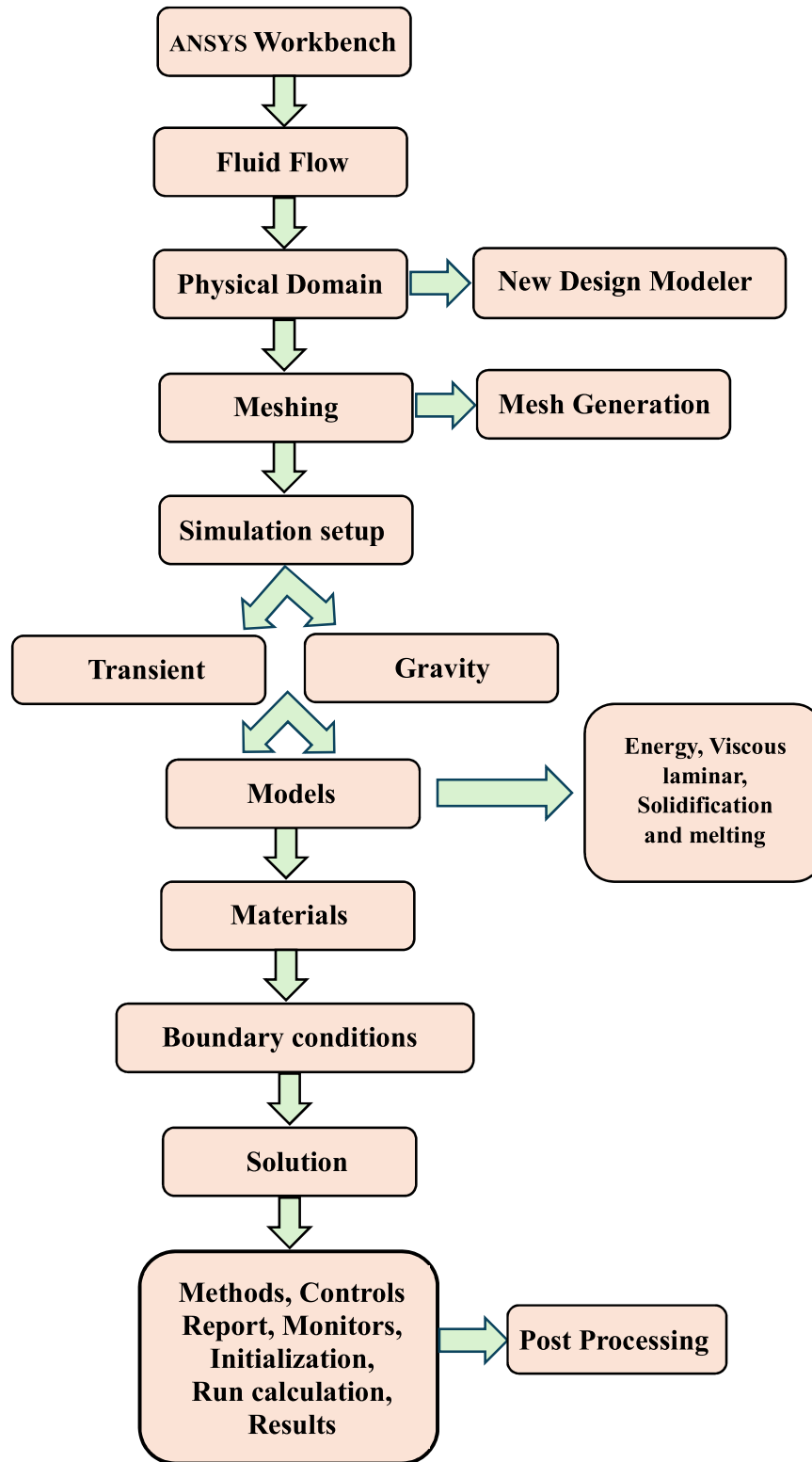


Fig. 2. Flow chart of the numerical approach.

incorporates the Boussinesq approximation to account for buoyancy effects, while also considering transient behavior and gravitational forces. The phase change phenomenon is modeled using the enthalpy-porosity approach, where the liquid fraction is treated as a porosity field within the computational domain. A second-order implicit scheme is employed for time discretization, and the SIMPLE algorithm is implemented to couple pressure and velocity fields. Pressure correction is handled using

the PRESTO scheme, while second-order upwind discretization is applied to the momentum and energy equations to enhance numerical accuracy. Additionally, a least-squares cell-based method is used for gradient computation. The solution is iterated until convergence is achieved, ensuring a residual tolerance of 10^{-6} for all variables. A time step of 0.1 s is maintained, with a maximum of 20 iterations per step to ensure computational stability and accuracy. The overall numerical

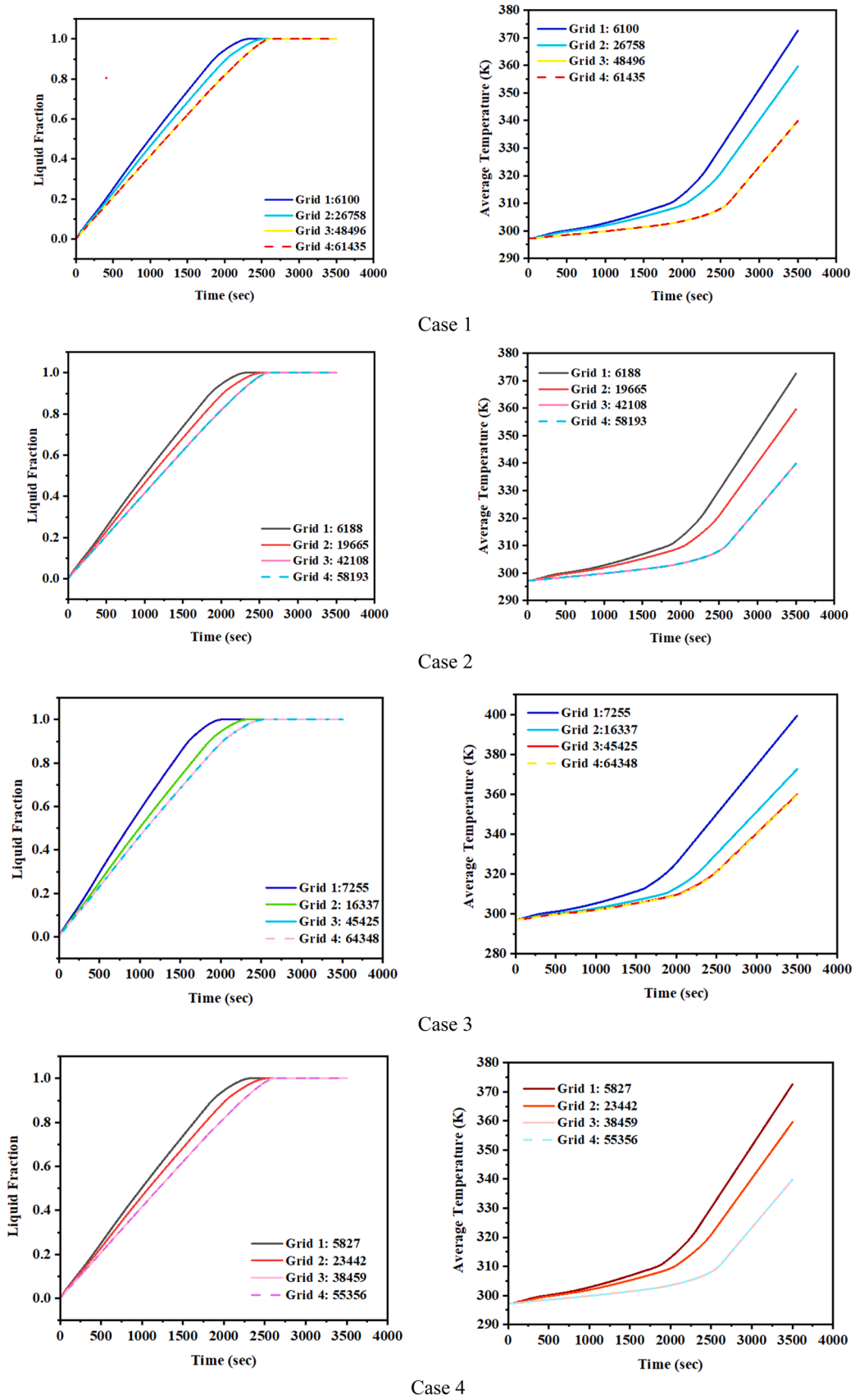


Fig. 3. Grid Independent Test results for liquid fraction and average temperature for different cases 1 to 4.

Table 1
Mesh statistics for Cases 1–4 (2D ANSYS Fluent).

Characteristic	Case-1 (Rectangular)	Case-2 (Triangular)	Case-3 (U- shaped)	Case-4 (Wavy)
Cells (elements)	47,289	41,076	43,022	35,410
Nodes	48,496	42,108	45,425	38,459
Planar domain area (mm ²)	575	575	574.9	574.9
Min element size (mm)	1.7889e-002	1.7889e-002	1.7889e- 002	1.7964e- 002
Max element size (mm)	1.79890	1.79890	1.79890	1.7812
Growth rate	1.20	1.20	1.20	1.20
Orthogonal quality (min)	0.51835	0.56699	0.44706	0.49565
Skewness (max)	0.74598	0.73855	0.75437	0.78462
Aspect ratio (max)	3.3089	3.1842	3.6366	3.5509

process is illustrated in Fig. 2.

3.1. Grid independent test

Grid independence tests are conducted for four different fin shapes mounted on the left wall of the enclosure, using aluminum fins. Four mesh resolutions are evaluated to assess grid sensitivity, incorporating wall refinement and various grid element types to examine the effect of element size on computational accuracy. The tests analyze the variation of average temperature (T_{avg}) and liquid fraction (LF) over time for each mesh configuration. As shown in Fig. 3, the results converge notably between Grids 3 and 4. The mesh configurations and other properties are presented in Table 1. Grid 3 was chosen because it strikes the optimal balance between computational accuracy and efficiency. Using Grid 4 would have increased computational cost and time without significant improvement in result accuracy, as the solution had already converged sufficiently at Grid 3. The advantage of Grid 3 lies in providing reliable and accurate results while keeping simulation resources manageable.

3.2. Validation

The simulation models for both finned and finless configurations are validated against experimental data provided by Bouzennada et al [31]. As illustrated in Fig. 4, the numerical predictions of heat energy and liquid fraction within the PCM region demonstrate strong agreement with the experimental observations across various time intervals. This

close correlation confirms the accuracy and robustness of the numerical approach, including the enthalpy-porosity method and applied boundary conditions. The validation enhances confidence in the model's ability to reliably simulate the thermal behavior of PCMs under different geometrical and thermal conditions, thereby supporting its use for further parametric investigation.

4. Results and discussion

4.1. Influence of fin geometry on melting behavior and liquid fraction

The thermal behavior of a dual-finned, two-dimensional enclosure filled with RT-27 phase change material (PCM) was investigated under a constant heat flux of 1000 W/m² for four cases: Case 1 (Rectangular), Case 2 (Triangular), Case 3 (U-shaped), and Case 4 (Wavy). The influence of fin shape on the melting rate and liquid fraction (LF) was evaluated at selected time intervals: 180 s, 600 s, 1200 s, 1800 s, and 2700 s, as presented in Fig. 5. A summary of the liquid fraction values at these intervals is provided in Table 2.

4.2. Early-Stage melting ($t = 180$ s)

At 180 s, melting begins locally around both the heated left-wall fin and the internal diagonal fin. Among all configurations, the U-shaped fin (Case 3) exhibits the most advanced melting, with an LF of approximately 0.15, attributed to its extended surface area and the promotion of convective flow paths. The rectangular fin (Case 1) follows closely with LF \approx 0.13, while the wavy fin (Case 4) and triangular fin (Case 2) show lower melting progress, with LFs of approximately 0.11 and 0.08, respectively. The inclusion of the diagonal fin enhances heat transfer deeper into the PCM, with the effect being particularly evident in the U-shaped and rectangular configurations.

4.3. Intermediate melting ($t = 600$ s)

As the simulation progresses, melting becomes more widespread. The U-shaped fin (Case 3) continues to outperform the other configurations, reaching LF \approx 0.40, with melting fronts expanding around both fins. The rectangular fin (Case 1) maintains strong performance with LF \approx 0.35, forming a broad melted zone through the enclosure's midsection. The wavy fin (Case 4) demonstrates moderate melting at LF \approx 0.29, while the triangular fin (Case 2) shows the slowest progress, with LF \approx 0.22. At this stage, the internal fin plays a vital role as a thermal bridge, distributing heat between the hot wall and the core of the PCM, with curved geometries (Cases 3 and 4) particularly benefiting from enhanced convective interactions.

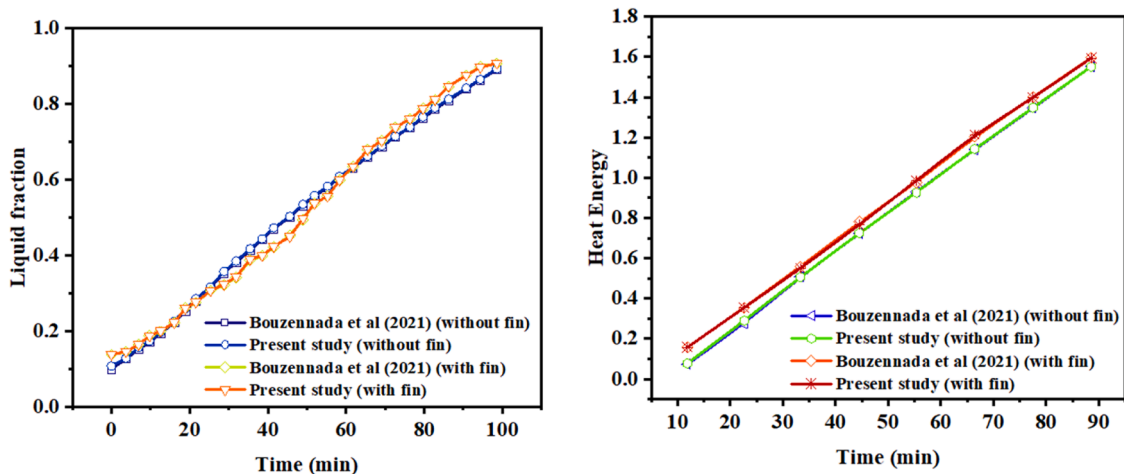


Fig. 4. Variation of liquid fraction and heat energy with time (min).

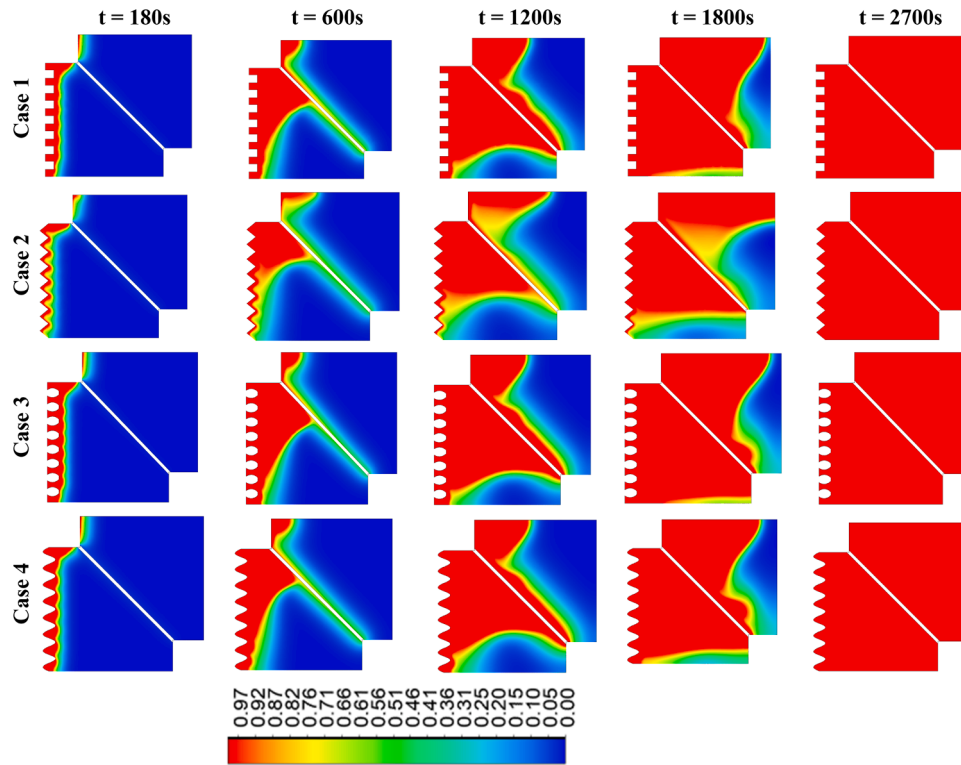


Fig. 5. Variation contour of LF for different types of fins with time, RT-27 and $Q = 1000 \text{ W/m}^2$.

Table 2

Summary of thermal performance.

Time (s)	Case 1: Rectangular	Case 2: Triangular	Case 3: U-shaped	Case 4: Wavy
180	~0.13	~0.08	~0.15	~0.11
600	~0.35	~0.22	~0.40	~0.29
1200	~0.61	~0.44	~0.70	~0.53
1800	~0.86	~0.70	~0.93	~0.78
2700	1.00	1.00	1.00	1.00

4.4. Accelerated phase transition ($t = 1200 \text{ s}$)

By 1200 s, a substantial portion of the PCM has transitioned to the liquid phase. The U-shaped fin continues to lead, achieving $LF \approx 0.70$, followed by the rectangular fin ($LF \approx 0.61$). The wavy and triangular fins show LFs of approximately 0.53 and 0.44, respectively. The superior performance of the U-shaped and rectangular fins is attributed to their structural ability to support multidirectional heat transfer and promote internal fluid motion. Although the rectangular fin achieves a relatively high liquid fraction, its melting pattern is less uniform. At 1200 s (Case 1), distinct unmelted regions persist on either side of the internal diagonal fin, indicating uneven heat distribution within the cavity.

4.5. Advanced melting ($t = 1800 \text{ s}$)

At this stage, melting is nearly complete in all configurations. The U-shaped fin (Case 3) achieves $LF \approx 0.93$, indicating near-complete melting. The rectangular fin (Case 1) follows with $LF \approx 0.86$, while the wavy (Case 4) and triangular (Case 2) fins reach LFs of ~ 0.78 and ~ 0.70 , respectively. The presence of the internal fin continues to be a critical factor in accelerating heat transfer, with the wavy geometry extending heat reach into remote zones. However, the triangular configuration consistently exhibits slower thermal progression, with notable stagnation zones.

4.6. Complete melting ($t = 2700 \text{ s}$)

By 2700 s, full melting ($LF \approx 1.0$) is achieved in all four cases. The U-shaped fin demonstrates the most efficient melting behavior throughout the entire process, driven by maximized contact area, effective heat spreading, and enhanced natural convection loops. The rectangular and wavy fins also perform effectively, though with slightly slower transition dynamics. In contrast, the triangular fin consistently shows slower and less uniform melting, particularly in the cavity's lower and central regions, reflecting less efficient thermal penetration.

4.7. Engineering implications

The results clearly indicate that fin geometry, particularly in conjunction with an internal diagonal fin, plays a critical role in accelerating the melting process, improving thermal uniformity, and enhancing overall energy storage efficiency. The U-shaped fin consistently outperforms the other configurations across all time intervals, offering faster melting, higher liquid fraction, and more complete thermal coverage. The wavy fin, while slightly slower, demonstrates excellent thermal distribution, reducing localized cold zones. The rectangular fin provides a solid balance of simplicity and effectiveness, whereas the triangular fin, with its limited heat transfer surface, remains the least effective in promoting uniform and rapid melting. These findings suggest that U-shaped and wavy fin geometries are optimal candidates for latent heat thermal energy storage systems, particularly in applications requiring rapid thermal response and efficient phase-change utilization.

4.8. Transient temperature distribution in dual-fin PCM enclosure

This section analyzes the transient temperature distribution within a dual-enclosure latent heat storage system filled with RT-27 phase change material (PCM) and subjected to a constant heat flux of 1000 W/m^2 for four geometries: Case 1 (Rectangular fin), Case 2 (Triangular fin),

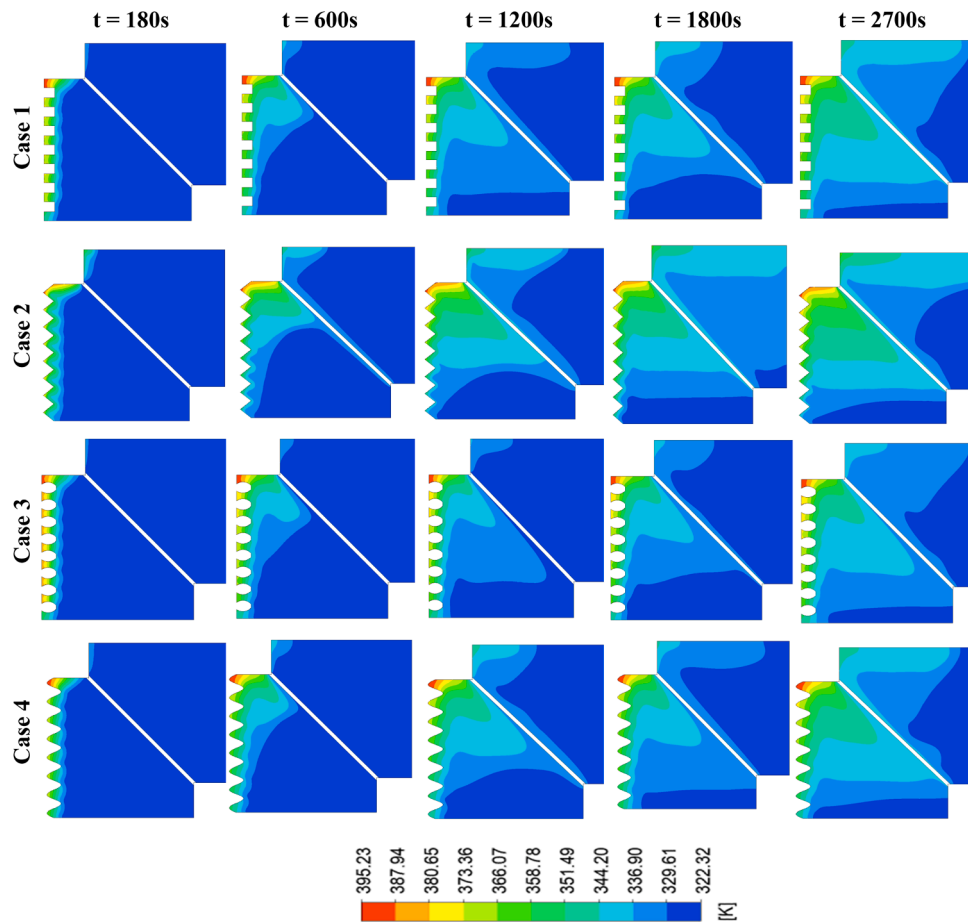


Fig. 6. Variation contour of Temperature for different types of fins with time, RT-27 and $Q = 1000 \text{ W/m}^2$.

Table 3
Maximum and Average Temperatures at 2700 s for Different Fin Configurations.

Fin Case	Max Temp (K)	Avg Temp (K)	Heat Penetration Speed	Thermal Uniformity	Performance Rank
Case 1: Rectangular	~393	~342	High	Very High	Best Overall
Case 2: Triangular	~385	~320	Low	Low	Least Effective
Case 3: U-shaped	~393	~365	Very High	Moderate	Best Overall
Case 4: Wavy	~393	~330	Moderate	Moderate	Moderate

Case 3 (U-shaped fin), and Case 4 (Wavy-shaped fin). The evolution of temperature fields at selected time intervals (180 s, 600 s, 1200 s, 1800 s, and 2700 s) is presented in Fig. 6. A summary of peak and average temperatures at 2700 s for each configuration is provided in Table 3.

4.9. Temperature rise and maximum values

Among all configurations, the U-shaped fin (Case 3) exhibits the highest thermal response, achieving a maximum temperature of approximately 393 K near the fin’s edge and an average cavity temperature of around 365 K. This indicates efficient heat distribution and deeper penetration of thermal energy across the domain.

The rectangular fin (Case 1) follows closely, also reaching a peak temperature of ~393 K, but with a lower average temperature of ~342 K, suggesting a slightly slower overall heat propagation despite localized heating effectiveness near the fin.

The wavy fin (Case 4) also reaches a maximum temperature of ~393 K, but its average temperature remains around 330 K, reflecting moderate performance. The fin’s extended geometry facilitates interaction

with the PCM but may delay uniform heat dispersion across the cavity.

The triangular fin (Case 2) demonstrates the least favorable performance, attaining a maximum temperature of only ~385 K and a lowest average cavity temperature of ~315 K at the end of the simulation period. This is due to its narrow profile and limited heat transfer surface, which reduce conductive and convective heat transport.

These findings confirm that U-shaped and rectangular fins promote superior heat propagation, while the triangular fin is less effective at transferring and maintaining elevated temperatures throughout the cavity—even after full melting is achieved. The quantitative comparison is summarized in Table 2.

4.10. Thermal uniformity and heat penetration

In terms of thermal uniformity, the rectangular fin (Case 1) shows the most balanced performance. It provides a consistent temperature field throughout the cavity, minimizing thermal gradients and hotspots. Although it reaches peak temperatures slightly slower than Case 3, its uniform and stable heating profile makes it highly suitable for

applications requiring precise thermal control, such as in electronics cooling or biomedical systems.

The U-shaped fin (Case 3) delivers the fastest and most intense heat transfer, driven by its extended branched surface that supports multidirectional conduction and natural convection loops. However, it also exhibits sharper temperature gradients, particularly near the fin surface. This makes it ideal for applications where rapid thermal response is more critical than temperature uniformity.

The wavy fin (Case 4) shows a more linear temperature gradient, with strong performance near the heated wall but relatively weaker propagation toward the far end of the cavity. While it ensures moderate uniformity, it does not fully utilize internal circulation as effectively as the U-shaped or rectangular designs.

The triangular fin (Case 2) remains the least effective in both heat transfer rate and temperature uniformity. Due to its limited surface area and tapered geometry, thermal penetration is slow, and cooler regions persist in the central and lower portions of the cavity.

The comparative results clearly demonstrate that fin geometry plays a critical role in determining the speed, reach, and distribution quality of

heat transfer in PCM enclosures. The U-shaped fin provides the fastest and most efficient heat transfer, making it highly effective for high-demand thermal storage and management systems. On the other hand, the rectangular fin offers superior thermal uniformity, which is advantageous for applications requiring consistent temperature regulation. Although the wavy fin exhibits only moderate overall performance, its extended undulating surface facilitates gradual heat dispersion, thereby reducing localized cold spots and promoting smoother temperature gradients. This observation is consistent with recent studies on sinusoidal wavy fins Kumar and Maurya [32], which report that while such fins may not achieve the fastest melting rates, they effectively enhance spatial thermal uniformity. The triangular fin, due to its weak heat transfer characteristics, may only be appropriate for low-priority or passive thermal management applications.

The diagonal fin serves as a conductive backbone that shortens the thermal path from the heated wall into the PCM core while also redirecting buoyant plumes. This dual action complements the wall-mounted fins, which expand surface area and generate vertical thermal plumes. In the early melting stage, the diagonal fin seeds multiple

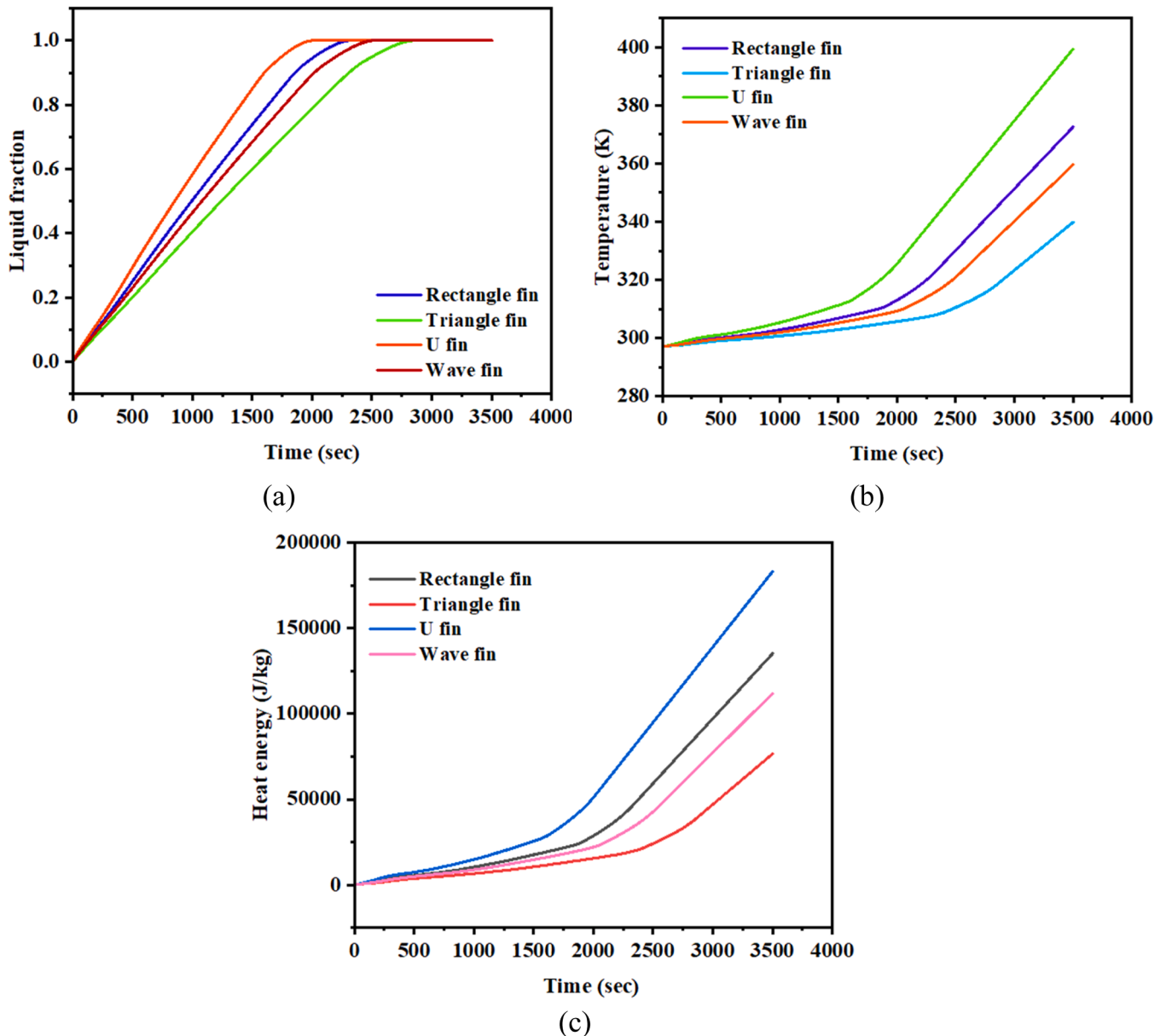


Fig. 7. Variation of (a) Liquid fraction and (b) Temperature (c) Heat energy with time for different fins at $Q = 1000 \text{ W/m}^2$.

melt fronts away from the heated wall, while in the convective stage it intercepts plumes and enhances circulation loops, thereby reducing stagnant cold pockets. During the final stage, when convection weakens, the diagonal fin sustains conduction and accelerates the complete melting of residual solids. These effects are most prominent in the U-shaped and rectangular geometries, where extended surface area on the wall side couples effectively with the diagonal bridge, yielding faster liquid-fraction growth and improved temperature uniformity (as evidenced in Figs. 5–6).

4.11. Quantitative analysis

4.11.1. Effects of fin geometry on melting, temperature distribution, and heat storage

The thermal performance of the dual-enclosure PCM system was investigated under a constant heat flux of 1000 W/m^2 , incorporating four distinct aluminum fin geometries—rectangular, triangular, U-shaped, and wavy. The presence of the internal fin contributes to enhancing thermal conductivity within the system by dispersing heat from the heated wall deeper into the PCM body. The effect of these geometries on melting behavior, temperature distribution, and thermal energy storage is analyzed and presented in Fig. 7.

4.11.2. Melting behavior

As shown in Fig. 7(a), the liquid fraction (LF) increases over time for all fin configurations, eventually reaching complete melting ($\text{LF} \approx 1.0$). However, the rate at which full melting occurs varies considerably across the designs. The U-shaped fin demonstrates the fastest melting performance, achieving complete phase change at approximately 2000 s. This is attributed to its optimized surface area and effective multidirectional heat distribution, which promote both conduction and convection within the PCM.

The rectangular fin follows, reaching full melting at around 2200 s, benefiting from its direct linear conduction path, even though its geometry is relatively simple. Interestingly, the wavy-shaped fin, despite having an extended contact surface that facilitates heat spreading, completes melting more gradually, around 2500 s. This slower response is likely due to the longer thermal paths and delayed heat penetration into distant regions of the cavity.

The triangular fin requires the longest time—approximately 2700 s—to fully melt the PCM. This delayed transition results from its narrow geometry and reduced effective heat transfer surface. These findings highlight the importance of fin geometry in determining melting efficiency, with the U-shaped configuration offering the most time-efficient solution—ideal for systems requiring rapid thermal response.

4.11.3. Temperature distribution

The average cavity temperature profiles after 3500 s, shown in Fig. 7(b), reveal a consistent trend with the melting performance. The U-shaped fin achieves the highest average temperature of approximately 400 K, confirming its strong thermal effectiveness. The rectangular fin reaches an average temperature of about 370 K, followed by the wavy fin at 360 K. The triangular fin again records the lowest thermal response, with an average temperature of only 340 K. These results suggest that geometries with curved or branched structures, such as the U-shaped and wavy fins, facilitate more effective heat dispersion throughout the PCM domain. This reduces localized cold spots, enhances temperature uniformity, and minimizes thermal resistance within the enclosure.

4.11.4. Energy storage

The thermal energy stored by the PCM after 3500 s is presented in Fig. 7(c). The data further reinforces the influence of fin geometry on system performance. The U-shaped fin results in the highest energy storage, with the PCM absorbing approximately 160 kJ/kg. The rectangular fin follows, storing around 130 kJ/kg. The wavy-shaped fin

stores 110 kJ/kg, and the triangular fin lags with only 75 kJ/kg. This progression demonstrates that enhanced surface contact and geometric complexity not only accelerate melting but also enable greater thermal energy absorption, crucial for maximizing the storage capacity of latent heat systems.

The results conclusively show that the combination of wall-mounted and internal diagonal fins, especially when utilizing geometries such as U-shaped or rectangular profiles, significantly improves the thermal performance of PCM enclosures. These designs:

- Promote multidirectional heat transfer,
- Enhance conduction and natural convection,
- Reduce thermal stratification and cold zones, and
- Support faster and more complete melting.

Among all cases, the U-shaped fin consistently outperforms others across all thermal metrics—melting rate, temperature rise, and energy storage—making it a highly suitable candidate for compact, efficient latent heat thermal energy storage systems. The rectangular fin provides a balance of simplicity and effectiveness, while the wavy fin ensures smoother, more uniform heating. In contrast, the triangular fin exhibits limited thermal reach and slower response, making it less favorable for high-performance applications.

4.11.5. Influence of heat flux levels on liquid fraction, temperature, and stored energy

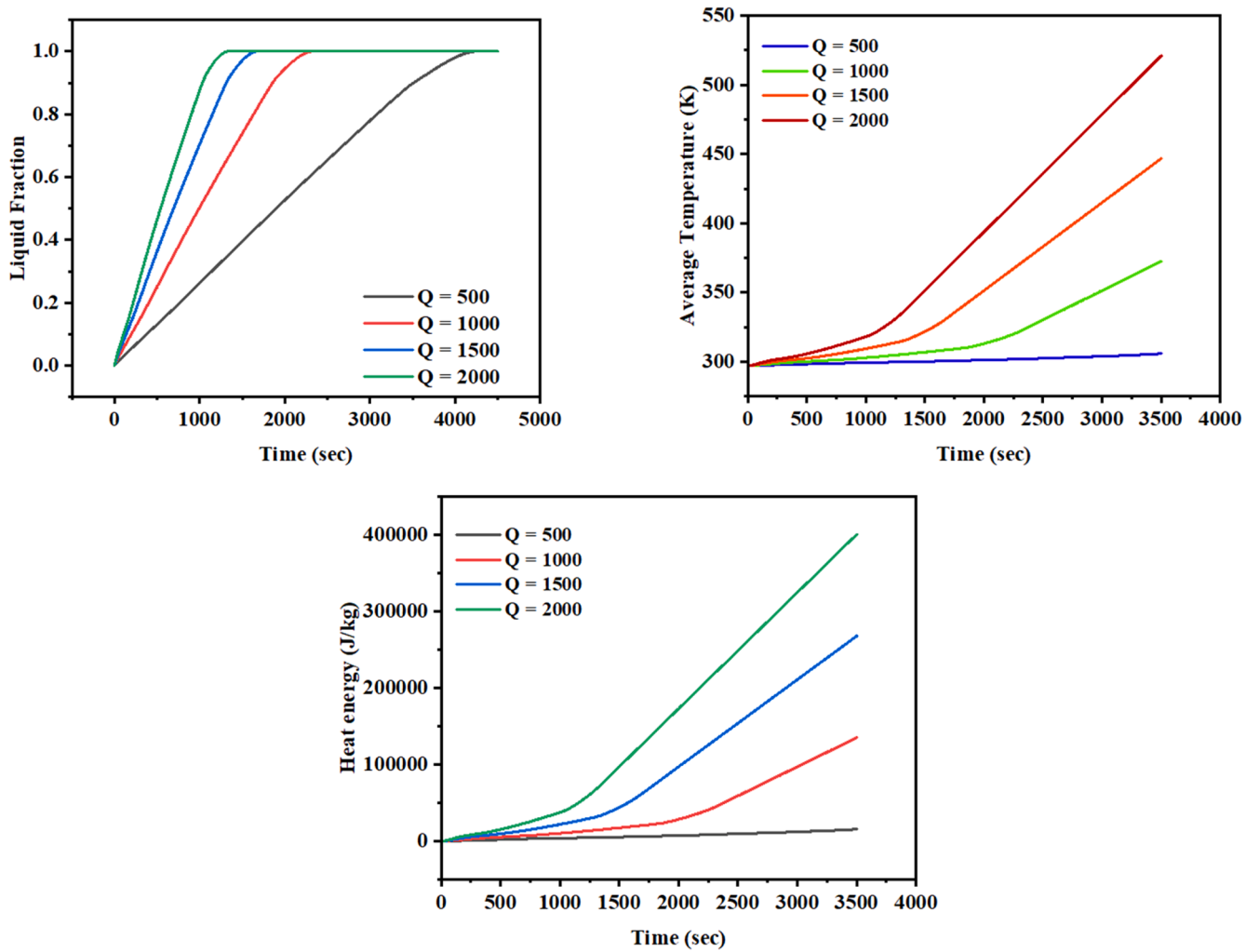
The thermal behavior of a dual-enclosure phase change material (PCM) system filled with RT-27 was systematically investigated under varying heat flux levels of 500, 1000, 1500, and 2000 W/m^2 . The analysis was conducted across four fin configurations—rectangular, triangular, U-shaped, and wavy-shaped—to evaluate their impact on thermal performance. Key performance indicators, including the melting time (defined as the time required to reach a liquid fraction of $\text{LF} = 1$), the average temperature of the PCM, and the stored thermal energy per unit mass, were assessed. The comparative results, as presented in Fig. 8, provide insight into the influence of heat flux intensity and fin geometry on the efficiency and responsiveness of the PCM-based thermal energy storage system.

4.11.6. Case 1: rectangular fin

The rectangular fin displays a consistent and linear thermal response to increasing heat flux. At 500 W/m^2 , full melting of the PCM is achieved in approximately 4500 s, which reduces significantly with higher fluxes to 2700, 1750, and 1450 s for 1000, 1500, and 2000 W/m^2 , respectively. This notable improvement is attributed to the fin's simple geometry, which supports efficient conduction along a direct path. The average PCM temperature increases from an initial 297 K to approximately 313, 375, 448, and 525 K, corresponding to the respective heat flux levels. Similarly, energy storage increases from 20 kJ/kg at 500 W/m^2 to 140, 275, and 400 kJ/kg at higher fluxes. These results indicate that the rectangular fin effectively responds to increased heat input, ensuring timely and complete phase change with substantial energy absorption.

4.11.7. Case 2: triangular fin

The triangular fin exhibits the least efficient thermal performance across all heat flux levels. At 500 W/m^2 , full melting occurs after about 5200 s, and although the melting time improves with higher heat fluxes, it remains longer than in other configurations—2850, 1850, and 1560 s for 1000, 1500, and 2000 W/m^2 , respectively. The average temperature rise is also relatively modest, reaching 311, 340, 400, and 455 K at increasing heat inputs. Correspondingly, energy storage remains lower, starting from 17 kJ/kg at 500 W/m^2 , and reaching 75, 175, and 275 kJ/kg at higher flux levels. The triangular shape's limited surface area and narrow tip reduce the effective conduction path, thereby slowing the overall heat distribution and PCM melting rate.



Case 1

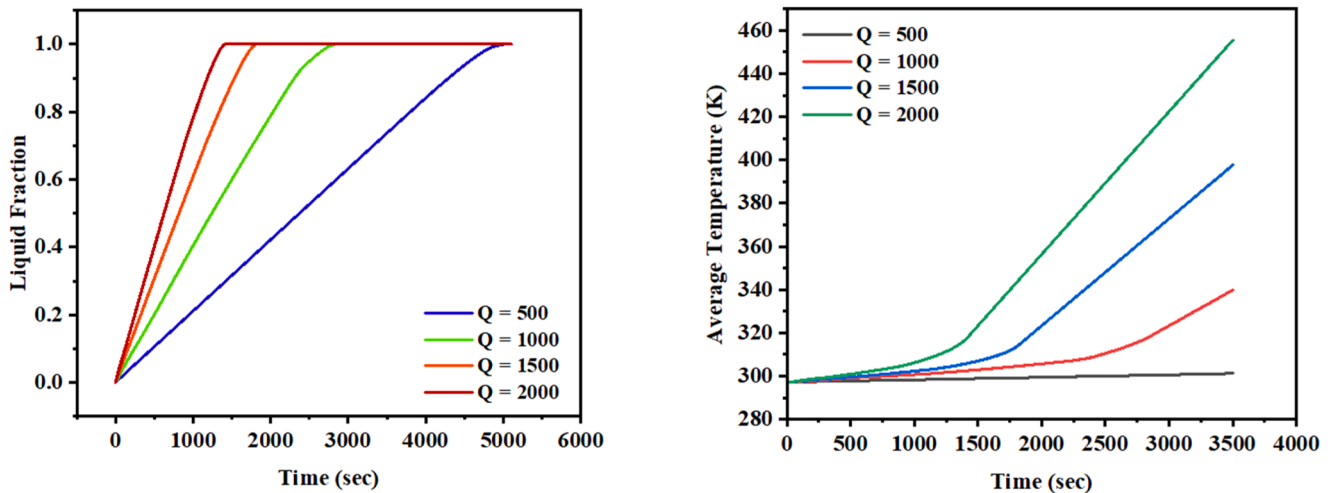


Fig. 8. Variation of liquid fraction, temperature and heat energy with time for different heat fluxes (W/m^2) and different fins.

4.11.8. Case 3: U-shaped fin

The U-shaped fin demonstrates superior thermal performance under all heat flux levels. Complete melting is achieved in the shortest durations across all conditions—4150, 2000, 1600, and 1400 s for 500 to 2000 W/m^2 , respectively. Its branched geometry and extended surface

area significantly enhance both conduction and natural convection within the enclosure.

The average PCM temperature rises steadily from 315 K at 500 W/m^2 to 350, 398, and 440 K at increasing heat fluxes. In parallel, the stored energy climbs from 23 kJ/kg at the lowest flux to 100, 175, and 279 kJ/

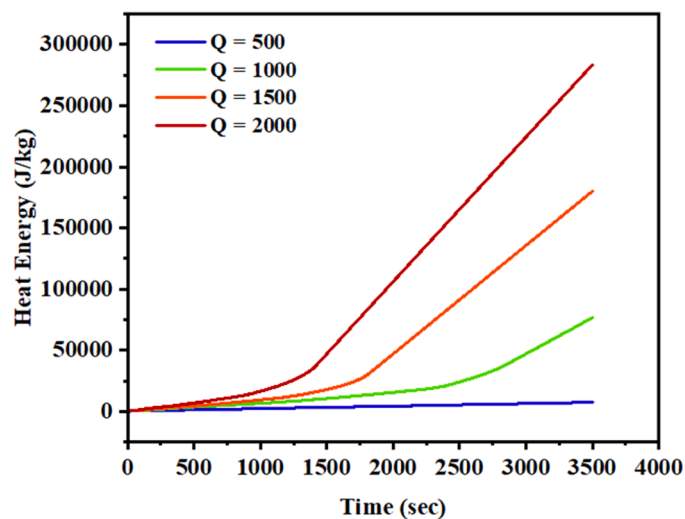
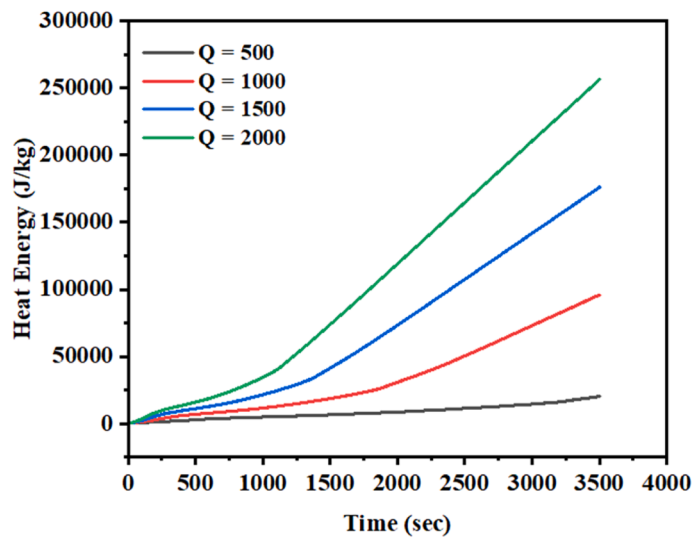
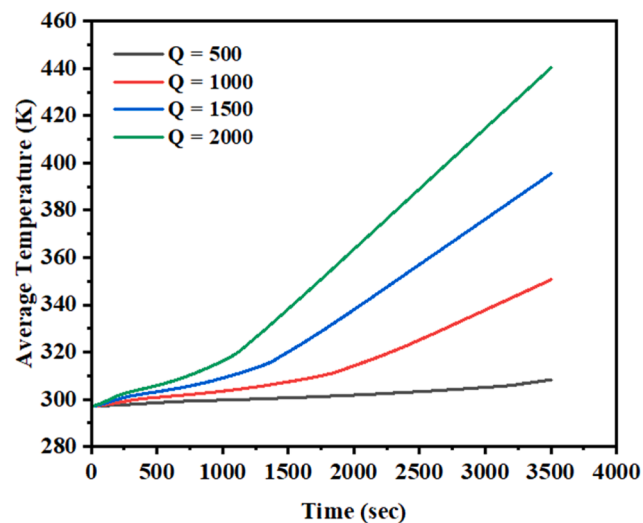
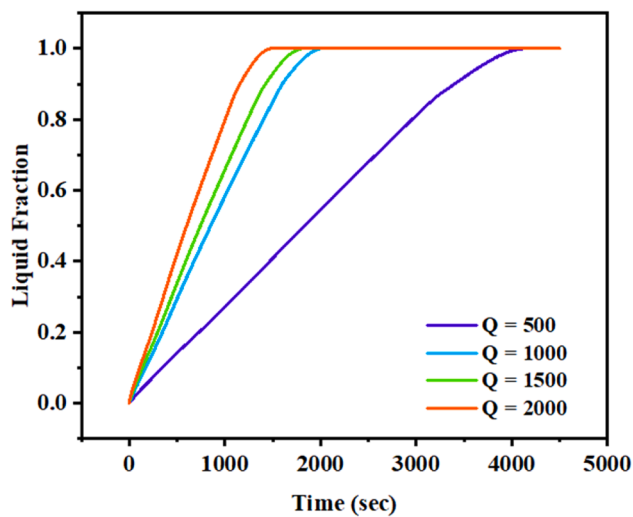
**Case 2****Case 3**

Fig. 8. (continued).

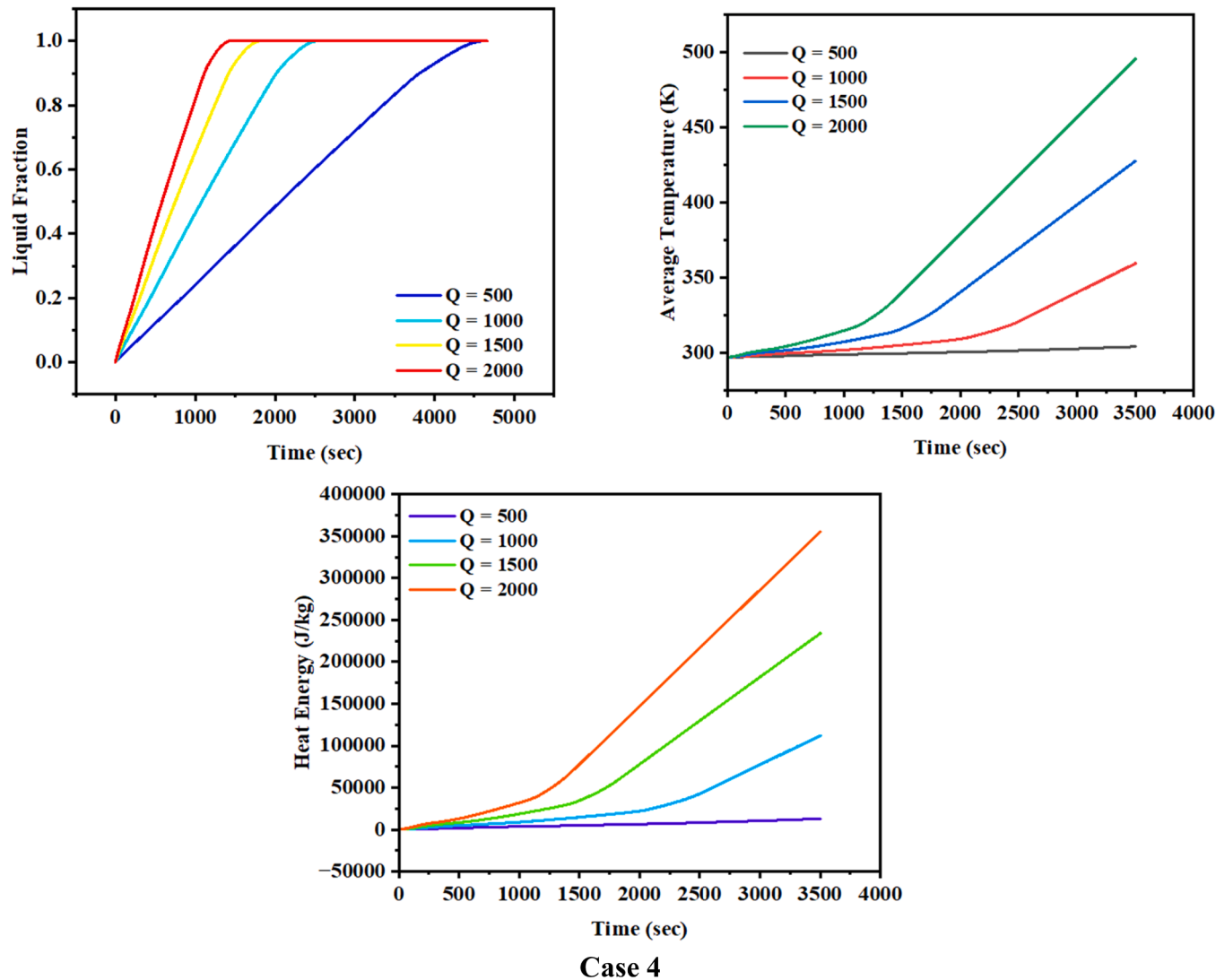


Fig. 8. (continued).

kg, reflecting the fin’s high energy utilization efficiency. The U-shaped design clearly offers the fastest melting and highest thermal performance across all metrics.

Table 4
Thermal performance metrics of all four fin configurations.

Heat Flux (W/m ²)	Fin Case	Melting Time (s)	Avg. Temp (K)	Energy Stored (kJ/kg)
500	Rectangular	4500	313	20
	Triangular	5200	311	17
	U-shaped	4150	315	23
	Wavy	4600	311.5	18
1000	Rectangular	2700	375	140
	Triangular	2850	340	75
	U-shaped	2000	350	100
	Wavy	2500	363	111
1500	Rectangular	1750	448	275
	Triangular	1850	400	175
	U-shaped	1600	398	175
	Wavy	1700	425	275
2000	Rectangular	1450	525	400
	Triangular	1560	455	275
	U-shaped	1400	440	279
	Wavy	1500	497	360

4.11.9. Case 4: wavy-shaped fin

The wavy-shaped fin exhibits a progressive and stable melting profile, characterized by uniform heat distribution and relatively fast thermal response. At 500 W/m², the PCM reaches complete melting in about 4600 s, while at 1000, 1500, and 2000 W/m², the times reduce to 2500, 1700, and 1500 s, respectively. The average temperature increases from 311.5 K to 363, 425, and 497 K across the rising heat flux values. Simultaneously, the thermal energy stored improves from 18 kJ/kg to 111, 275, and 360 kJ/kg. Although slightly slower than the U-shaped fin, the wavy fin ensures more uniform thermal fields, reducing localized overheating and enhancing temperature stability within the PCM. Table 4 below summarizes the thermal performance metrics of all four fin configurations across the tested heat fluxes:

The results underscore the crucial role of fin geometry and heat flux in determining the thermal performance of PCM enclosures. Increasing heat flux substantially reduces melting time, raises the average PCM temperature, and boosts the total energy stored, across all configurations. Among the fins, the U-shaped geometry (Case 3) delivers the fastest melting, making it the most effective design for rapid thermal management systems. The wavy fin (Case 4), though slightly slower, offers excellent temperature uniformity, beneficial for applications requiring stable and controlled heat distribution.

The rectangular fin (Case 1) performs moderately well with a predictable conduction path and good scalability under increasing heat

flux. In contrast, the triangular fin (Case 2) consistently underperforms due to its limited heat transfer surface and weak thermal reach. In conclusion, for systems prioritizing speed and energy efficiency, the U-shaped fin is the optimal choice. For uniform temperature fields and thermal stability, the wavy-shaped fin offers a reliable alternative. These insights can directly guide the design of thermal energy storage units, electronics cooling systems, and biomedical thermal devices.

4.11.10. Comparative analysis and benchmarking

The performance differences mainly come from conduction paths and how each fin shape drives natural convection. The U-shaped fin offers multiple contact edges and curved channels that guide upward plumes, giving the fastest melting (~ 2000 s at 1000 W/m^2) and highest energy ($\sim 160 \text{ kJ/kg}$). The rectangular fin creates a straight conduction path and a stable plume, leading to uniform temperature fields and only slightly longer melting (~ 2700 s). The wavy fin adds surface area, producing smoother heat distribution but slower penetration than U or rectangular fins. The triangular fin has limited tip area and weak plume circulation, which traps cold PCM and results in the lowest performance ($\sim 75 \text{ kJ/kg}$). The internal diagonal fin plays a key role: it seeds extra melt fronts and redirects plumes across the core, which shortens melt time and reduces stagnant regions, especially in the U and rectangular designs.

Recent works on fin design show melting-time reductions of 14–33 % [3,15,32]. In comparison, this study finds that the U-shaped fin with a diagonal bridge reduces melting time by ~ 26 % compared to the triangular design under identical heat flux, while also delivering the highest stored energy. The rectangular and wavy fins perform between these extremes, with rectangular giving the most uniform temperature field and wavy producing smoother but slower heat penetration. Unlike many earlier studies that assume isothermal boundaries, this work uses constant heat fluxes (500 – 2000 W/m^2), showing consistent performance rankings across practical operating loads. With the dual-enclosure configuration and diagonal conduction path, the system demonstrates both faster charging and higher energy storage compared with common single-fin geometries in the literature.

5. Limitations

The simulation employs a two-dimensional model, which may not fully capture the three-dimensional heat transfer effects, especially in real-world PCM enclosures where 3D conduction and convection can significantly influence performance. The study assumes constant thermophysical properties for both PCM and aluminum fins throughout the phase change process. In practice, these properties may vary with temperature, potentially affecting accuracy. The volume change of the PCM during melting is ignored, which could influence pressure and flow fields in actual systems and affect the design of containment structures.

Only four static fin shapes are considered (rectangular, triangular, U-shaped, and wavy). More complex or hybrid fin designs, orientations, and dynamic fin structures are not explored.

6. Conclusion

This study provides a comprehensive numerical investigation into the influence of fin geometry and heat flux on the thermal performance of a chamfered dual-enclosure latent heat thermal energy storage (LHTES) system using RT-27 phase change material (PCM). Four aluminum fin geometries—rectangular, triangular, U-shaped, and wavy—were analyzed under varying heat fluxes of 500 , 1000 , 1500 , and 2000 W/m^2 using the enthalpy–porosity method implemented in ANSYS Fluent.

Among the configurations, the U-shaped fin consistently demonstrated superior thermal performance across all metrics. At 1000 W/m^2 , it achieved full melting in just 2000 s, reached the highest average cavity temperature of 365 K , and stored the maximum thermal energy of

approximately 160 kJ/kg . The rectangular fin also exhibited strong performance with efficient heat conduction and excellent thermal uniformity. The wavy fin offered moderate results with improved thermal distribution, while the triangular fin consistently underperformed due to its limited heat transfer surface and geometry.

Increasing the heat flux significantly accelerated melting times across all fin types. At 2000 W/m^2 , the U-shaped fin achieved complete melting in only 1400 s and showed the most efficient energy absorption profile. The comparative analysis confirmed that the combination of a wall-mounted and internal diagonal fin, particularly in U-shaped or rectangular forms, can significantly enhance melting rate, heat penetration, and energy storage efficiency.

These insights offer valuable design guidance for developing compact, high-performance LHTES systems. Future work may explore the integration of nanomaterials, hybrid fins, and dynamic boundary conditions to further optimize PCM-based thermal management solutions in real-world applications such as solar thermal systems, electronics cooling, and biomedical devices.

Use of AI

The authors used AI-assisted technology (ChatGPT 3.5) for language editing and grammar checking.

CRediT authorship contribution statement

Vignesh Elangovan: Writing – review & editing, Writing – original draft, Visualization, Validation, Software, Methodology, Investigation, Formal analysis. **Ramanipriya Mahalingam:** Writing – review & editing, Writing – original draft, Investigation, Formal analysis. **Mohammad Junaid:** Writing – review & editing, Writing – original draft. **Goutam Saha:** Writing – review & editing, Writing – original draft, Supervision, Conceptualization.

Declaration of competing interest

Authors declare No conflict of Interest

Funding

It's a self-funded research.

Data availability

All data are available in the article.

References

- [1] C. Zhao, J. Wang, Y. Sun, S. He, K. Hooman, Fin design optimization to enhance PCM melting rate inside a rectangular enclosure, *Appl. Energy* 321 (2022) 119368, <https://doi.org/10.1016/j.apenergy.2022.119368>. Article.
- [2] R. De Césaro Oliveski, F. Becker, L.A.O. Rocha, C. Biserni, G.E.S. Eberhardt, Design of fin structures for phase change material (PCM) melting process in rectangular cavities, *J. Energy Storage* 35 (2021) 102337, <https://doi.org/10.1016/j.est.2021.102337>. Article.
- [3] S.A. Kadhim, K.A. Hammoodi, M.J. Alshukri, I. Omle, K.K.A. Hussein, A.F. Khalaf, A. Elsheikh, Enhancing the melting rate of RT42 paraffin wax in a square cell with varied copper fin lengths and orientations: a numerical simulation, *Int. J. Thermofluids* 24 (2024) 100877, <https://doi.org/10.1016/j.ijft.2024.100877>. Article.
- [4] H.-T. Chen, R.-X. Zhang, W.-M. Yan, M. Amani, T. Ochoidek, Numerical and experimental study of inverse natural convection heat transfer for heat sink in a cavity with phase change material, *Int. J. Heat. Mass Transf.* 224 (2024) 125333, <https://doi.org/10.1016/j.jheatmasstransfer.2024.125333>. Article.
- [5] P. Rawat, Ashwni, A.F. Sherwani, A numerical study on the impact of fin length arrangement and material on the melting of PCM in a rectangular enclosure, *Int. J. Heat. Mass Transf.* 205 (2023) 123932, <https://doi.org/10.1016/j.jheatmasstransfer.2023.123932>. Article.
- [6] A.O. Elsayed, Numerical investigation on PCM melting in triangular cylinders, *Alex. Eng. J.* 57 (4) (2018) 2819–2828, <https://doi.org/10.1016/j.aej.2018.01.005>.

- [7] Y. Hong, Y. Shi, F. Li, F. Guo, D. Bai, J. Du, Energy storage and heat transfer characteristics of multiple phase change materials in a rectangular cavity with different layouts of T-shaped fins, *Int. Commun. Heat Mass Transf.* 159 (2024) 108068, <https://doi.org/10.1016/j.icheatmasstransfer.2024.108068>. Article.
- [8] N.A.A. Qasem, A. Abderrahmane, A. Belazreg, O. Younis, Y. Khetib, K. Guedri, Investigation of phase change heat transfer in a rectangular case as function of fin placement for solar applications, *Case Stud. Therm. Eng.* 54 (2024) 103996, <https://doi.org/10.1016/j.csite.2024.103996>. Article.
- [9] B. Kiyak, H.F. Öztop, N. Biswas, H. Coşanay, F. Selimefendil, Effects of fin shapes and orientations with cyclic heating and cooling on melting and solidification of PCM-filled closed space, *Int. J. Heat. Fluid. Flow.* 112 (2025) 109753, <https://doi.org/10.1016/j.ijheatfluidflow.2025.109753>.
- [10] G. Czerwinski, J. Woloszyn, Partitions influence on rectangular latent heat thermal energy storage unit performance during melting and solidification, *Int. Commun. Heat Mass Transf.* 159 (2024) 108047, <https://doi.org/10.1016/j.icheatmasstransfer.2024.108047>.
- [11] M. Barthwal, D. Rakshit, No fins attached? Numerical analysis of internal-external fins coupled PCM melting for solar applications, *Appl. Therm. Eng.* 215 (2022) 118911, <https://doi.org/10.1016/j.applthermaleng.2022.118911>. Article.
- [12] L. Tan, Y. Kwok, A. Date, A. Akbarzadeh, Numerical study of natural convection effects in latent heat storage using aluminum fins and spiral fillers, *Proc. World Acad. Sci. Eng. Technol.* 68 (2012) 518.
- [13] Z. Zhao, B. Hu, J. He, M. Lin, H. Ke, Effect of fin shapes on flow boiling heat transfer with staggered fin arrays in a heat sink, *Appl. Therm. Eng.* 225 (2023) 120179, <https://doi.org/10.1016/j.applthermaleng.2023.120179>.
- [14] K.A. Hammoodi, S.A. Kadhim, D.R. Nayyaf, K.K.A. Hussein, Z.I. Mohammed, A. H. Askar, I. Omle, A.F. Khalaf, H.Q. Hussein, Investigation of the influence of the air layer on the phase change material melting process inside a hemicylindrical enclosure: a numerical approach, *Results. Eng.* 24 (2024) 103337, <https://doi.org/10.1016/j.rineng.2024.103337>. Article.
- [15] Y. Zhang, B. Sun, X. Zheng, P.K. Singh, H. Ayed, A. Mouldi, A. Mohamed, S. Mehrez, Investigation on effect of connection angle of "L" shaped fin on charging and discharging process of PCM in vertical enclosure, *Case Stud. Therm. Eng.* 33 (2022) 101908, <https://doi.org/10.1016/j.csite.2022.101908>.
- [16] H.-Y. Liu, Y.-P. Hu, G.-Y. Yang, C.-M. Wu, Y.-R. Li, PCM melting characteristics in a sidewall-heated rectangular cavity with non-uniform longitudinal fins near the bottom, *Renew. Energy* 242 (2025) 122451, <https://doi.org/10.1016/j.renene.2025.122451>. Article.
- [17] B. Kiyak, H.F. Öztop, N. Biswas, F. Selimefendil, Effects of geometrical configurations on melting and solidification processes in phase change materials, *Appl. Therm. Eng.* 258 (2025) 124726, <https://doi.org/10.1016/j.applthermaleng.2024.124726>. Article.
- [18] M.F. Osman, K.P. Sarath, M. Deepu, Studies on the melting dynamics of PCM in a semicircular cavity with straight and wavy heating surfaces, *Int. Commun. Heat Mass Transf.* 151 (2024) 107249, <https://doi.org/10.1016/j.icheatmasstransfer.2024.107249>. Article.
- [19] A. Rahmani, M. Dibaj, M. Akrami, Computational investigation of magnetohydrodynamic flow and melting process of phase change material in a battery pack using the lattice Boltzmann method, *J. Energy Storage* 78 (2024) 110046, <https://doi.org/10.1016/j.est.2023.110046>. Article.
- [20] H.-Y. Liu, L. Zhang, C.-M. Wu, Y.-R. Li, Comprehensive investigation of a novel latent energy storage unit exhibiting enhanced natural convection, *Int. J. Heat. Mass Transf.* 219 (2024) 124911, <https://doi.org/10.1016/j.ijheatmasstransfer.2023.124911>. Article.
- [21] V.A. Wagh, S.K. Saha, Optimising extended fin design and heat transfer coefficient for improved heat transfer and PCM recover time in thermal management of batteries, *Appl. Therm. Eng.* 255 (2024) 123964, <https://doi.org/10.1016/j.applthermaleng.2024.123964>. Article.
- [22] F. Souayfane, F. Fardoun, P.-H. Biwolé, Phase change materials (PCM) for cooling applications in buildings: a review, *Energy Build.* 129 (2016) 396–431, <https://doi.org/10.1016/j.enbuild.2016.04.006>.
- [23] A. Nejman, M. Cieślak, The impact of the heating/cooling rate on the thermoregulating properties of textile materials modified with PCM microcapsules, *Appl. Therm. Eng.* 127 (2017) 212–223, <https://doi.org/10.1016/j.applthermaleng.2017.08.037>.
- [24] S. Bista, S.E. Hosseini, E. Owens, G. Phillips, Performance improvement and energy consumption reduction in refrigeration systems using phase change material (PCM), *Appl. Therm. Eng.* 142 (2018) 723–735, <https://doi.org/10.1016/j.applthermaleng.2018.07.068>.
- [25] S. Lee, H. Choi, P. Park, S. Kang, K. Choi, H. Lee, Investigation of enhanced PCM heat sink design under extreme thermal conditions for high-heat-generating electronic devices, *Int. Commun. Heat Mass Transf.* 159 (2024) 108050, <https://doi.org/10.1016/j.icheatmasstransfer.2024.108050>. Article.
- [26] T. Ahmed, M. Bhourli, D. Groulx, M.A. White, Passive thermal management of tablet PCs using phase change materials: continuous operation, *Int. J. Therm. Sci.* 134 (2018) 101–115, <https://doi.org/10.1016/j.ijthermalsci.2018.08.010>.
- [27] P. Marin, M. Saffari, A. de Gracia, X. Zhu, M.M. Farid, L.F. Cabeza, S. Ushak, Energy savings due to the use of PCM for relocatable lightweight buildings passive heating and cooling in different weather conditions, *Energy Build.* 129 (2016) 274–283, <https://doi.org/10.1016/j.enbuild.2016.08.007>.
- [28] N.S. Bondareva, M.A. Sheremet, Conjugate heat transfer in the PCM-based heat storage system with finned copper profile: application in electronics cooling, *Int. J. Heat. Mass Transf.* 124 (2018) 1275–1284, <https://doi.org/10.1016/j.ijheatmasstransfer.2018.04.040>.
- [29] M. Junaid, G. Saha, P. Shahrear, S.C. Saha, Phase change material performance in chamfered dual enclosures: exploring the roles of geometry, inclination angles and heat flux, *Int. J. Thermofluids* 24 (2024) 100919, <https://doi.org/10.1016/j.ijft.2024.100919>. Article.
- [30] M. Junaid, G. Saha, P. Shahrear, S.C. Saha, Numerical evaluation of a dual phase change material-integrated cap for prolonged thermal protection in extreme heat, *Results. Eng.* (2025) 105870, <https://doi.org/10.1016/j.rineng.2025.105870>.
- [31] T. Bouzennada, F. Mechighel, T. Ismail, L. Kolsi, K. Ghachem, Heat transfer and fluid flow in a PCM-filled enclosure: effect of inclination angle and mid-separation fin, *Int. Commun. Heat Mass Transf.* 124 (2021) 105280, <https://doi.org/10.1016/j.icheatmasstransfer.2021.105280>. Article.
- [32] A. Kumar, A. Maurya, Transient analysis of phase change material-based triple-tube unit with sinusoidal wavy-shaped fin, *Arab. J. Sci. Eng.* 49 (8) (2024) 10867–10889, <https://doi.org/10.1007/s13369-023-08525-x>.